

## Theoretical Studies of the Insertion of Carbenes in the Zeolite Framework: Modification of the Acidity and Creation of Chiral Sites

Maria Beatriz S. Mota,<sup>a</sup> Nilton Rosenbach Jr.<sup>b,c</sup> and Claudio J. A. Mota<sup>\*a,c</sup>

<sup>a</sup>Instituto de Química, Universidade Federal do Rio de Janeiro (UFRJ),  
Av. Athos da Silveira Ramos 149, CT Bl. A, 21941-909 Rio de Janeiro-RJ, Brazil

<sup>b</sup>Centro Universitário Estadual da Zona Oeste (UEZO),  
Av. Manuel Caldeira de Alvarenga, 1203, 23070-200 Campo Grande-RJ, Brazil

<sup>c</sup>INCT Energia e Ambiente, Universidade Federal do Rio de Janeiro (UFRJ),  
21941-909 Rio de Janeiro-RJ, Brazil

Foi realizado um estudo teórico da inserção de carbenos (CH<sub>2</sub> e CHCHO) na estrutura cristalina da zeólita Y. O método *our own n-layered integrated molecular orbital and molecular mechanics* (ONIOM) M062x/6-31G(d,p):PM6 foi utilizado para descrever a inserção do metileno (CH<sub>2</sub>) nas ligações T–O (T = Si ou Al) da rede resultando em quatro estruturas isômeras. Em todos os casos os cálculos indicaram uma alta exotermicidade para a inserção do metileno na rede cristalina, independentemente da multiplicidade do carbeno (singleto ou tripleto). A inserção na ligação O–H ácida para formar um grupo metóxi adsorvido foi o processo mais favorável, mas este caminho não ocorre se a inserção é feita na zeólita desprotonada. A inserção do formil-carbeno (CHCHO) cria centros quirais na estrutura cristalina. A acidez da zeólita após a inserção dos carbenos foi calculada usando a energia de desprotonação. Os cálculos predizem a possibilidade de desenvolver zeólitas ácidas com centros quirais, que poderiam imitar enzimas, especialmente para uso em processos de química fina e transformação de biomassa.

A theoretical study of the insertion of carbenes (CH<sub>2</sub>, CHCHO) in the framework structure of zeolite Y was carried out. The “our own n-layered integrated molecular orbital and molecular mechanics” (ONIOM) scheme M062x/6-31G(d,p):PM6 was used to describe the insertion of methylene (CH<sub>2</sub>) in the T–O bonds (T = Si, Al) of the framework yielding four isomeric structures. In all cases, calculations indicated a high exothermic process for the insertion of methylene in the framework, regardless of the spin multiplicity of the carbene (singlet or triplet). Insertion into the acidic O–H bond to afford an adsorbed methoxy group was the most favourable process, but this pathway does not occur if insertion is carried out on the deprotonated zeolite. Insertion of formylcarbene (CHCHO) creates chiral sites in the framework. The acidity of the zeolite structures after carbene insertion was calculated by means of the deprotonation energy. The calculations predicted the possibility of designing acidic zeolites with chiral sites that could mimic enzymes, especially for uses in fine chemical processes and biomass transformations.

**Keywords:** zeolites, acidity, carbene, theoretical calculations, chirality

### Introduction

Zeolites are crystalline aluminosilicates with pores of molecular dimension. They are important catalysts in the petrochemistry sector, due to their acidic and shape selective properties.<sup>1</sup> Since the pioneer use of zeolites in hydrocarbon cracking,<sup>2,3</sup> the modification of their acidity

has been a long standing goal of research. It has been found that catalytic activity is mainly affected by the Si/Al ratio,<sup>4,5</sup> presence of extra-framework aluminium species (EFAL),<sup>6</sup> presence of high valence cations<sup>7,8</sup> and isomorphic substitution.<sup>9</sup> Different zeolite structures also present different catalytic behaviour, which has been associated with their acid strength, but studies<sup>10</sup> of microcalorimetry of amine adsorption does not support such interpretation.

\*e-mail: cmota@iq.ufrj.br

The measurement of zeolite acid strength is still a matter of debate.<sup>11</sup> Different techniques have compared the acid strength of zeolite with the acidity of concentrated sulfuric acid solutions.<sup>12-14</sup> Despite the traditional use of zeolites in cracking, isomerisation and alkylation of hydrocarbons, their use in fine chemistry and biomass transformation is gaining increased attention,<sup>15</sup> which makes the understanding of the factors that governs zeolite acidity a still actual subject, especially at molecular level.

The acid site of a zeolite may be simply described as the interaction of a silanol group with a tricoordinated adjacent aluminium atom. The proton is covalently bonded to a bridge oxygen atom forming a zwitterion. This simple molecular arrangement can be affected by the zeolite framework structure, which influences the angles and bond length, by the presence of adjacent extra-framework species, which may disturb the electronic density near the acid site and by isomorphous substitution, which may influence the local geometry, as well as the electronic density.

The use of computational techniques to study the catalytic phenomenon has gained worldwide interest in the past decades.<sup>16,17</sup> The understanding of the nature of active sites<sup>18,19</sup> and the adsorption process at molecular level,<sup>20</sup> as well as the study of the reaction mechanism with description of intermediates<sup>21-23</sup> and calculation of activation parameters,<sup>24,25</sup> are some of the contributions of molecular modelling to the field of catalysis. However, the design of new and improved catalysts with the help of computation is still a distant target. Part of the problem relies on the lack of comprehension of the catalytic process at molecular level, which may inspire the design of improved materials.

In this article we wish to show that hybrid calculations, using quantum mechanics (QM)/QM(semiempirical) approach, can be used to explore new approaches of modifying the zeolite acidity. We studied the insertion of carbenes<sup>26</sup> in the framework of the zeolite (T–O bond). The idea is to create local geometric constraint in the neighbourhood of the acid site, as well as electronic perturbations that may influence the acidity. In addition, depending on the structure of the carbene, chiral sites may be created in the framework, which may be further explored in asymmetric catalysis. The theoretical results can predict the behaviour of the modified zeolite structure, helping the design of improved catalysts, which may be further synthesized in the laboratory to test their predicted performance.

## Methodology

The “our own n-layered integrated molecular orbital and molecular mechanics” (ONIOM) scheme<sup>27</sup> is one of

the most popular hybrid methods. It has been shown to correctly reproduce the properties of the Brønsted acid sites in ZSM-5 zeolite<sup>28</sup> and the study of proton transfer in zeolite-catalysed reactions.<sup>29</sup>

A cluster model (Figure 1) of the zeolite Y comprising 288 atoms ( $\text{Si}_{84}\text{O}_{132}\text{H}_{72}$ ), corresponding to two coupled supercavities, was obtained from the crystallographic coordinates available in the literature.<sup>30</sup> In order to avoid dangling bonds, the free valences of the border silicon atoms were saturated with hydrogen atoms located at 1.09 Å distance and in the same plane of the Si–O bond. The position of the hydrogen atoms was kept fixed during the optimisation steps, to avoid topological distortion of the model compared to the original zeolite Y structure. The aluminium atom and the organic moiety were inserted afterwards. We choose the  $\text{O}_1$  position to bond with the proton, because this position is one of the most preferred positions according to neutron scattering studies<sup>31</sup> and theoretical calculations.<sup>32</sup> Calculations of the structure of the acidic zeolite and the free carbene were also carried out to obtain the thermodynamics profile.

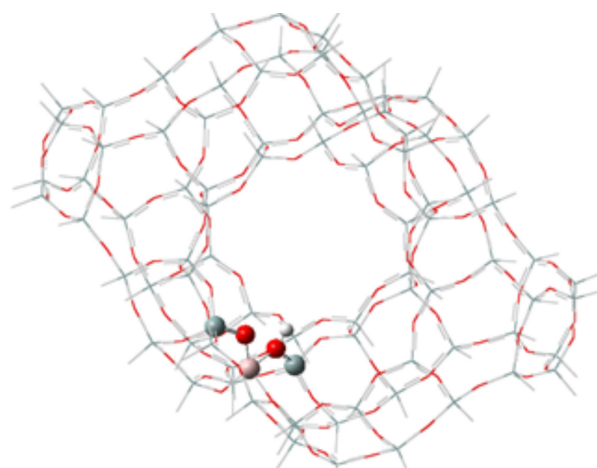


**Figure 1.** Framework structure of the zeolite Y used in calculations at ONIOM (M062x/6-31G(d,p):PM6) level. The high layer is represented by balls and accounts for Si–O–Al–OH–Si site. The lower layer is displayed in sticks and accounts for Si–O bonds with hydrogen atoms at terminations to avoid dangling bonds.

All calculations were done using the ONIOM method available in GAUSSIAN 09 package.<sup>33</sup> In the optimisation steps, the system was divided in two layers (high and low layers) and the atoms of the  $\text{T}_3$  cluster model and the organic moiety (high layer) were treated at the M062x/6-31(d,p) level, whereas the rest of the zeolite cavity (low layer) was treated by the semiempirical PM6 method. Vibrational analysis in the harmonic approximation (HO) was performed for all calculated structures at ONIOM(M062x/6-31(d,p):PM6) level and

corrected for the zero-point energy (ZPE) and thermal effects (298.15 K). Small imaginary frequencies related to the fixed hydrogen atoms were not considered in these calculations. To ascertain the acid strength of the structures, the deprotonation energy was calculated at the same level of theory. All energy data refer to the enthalpic term at 298.15 K and 1 atm and do not take into account translational, rotational and pV contributions.

## Results and Discussion

### Thermodynamics of carbene insertion

We initially calculated the insertion of methylene ( $\text{CH}_2$ ) into the T–O bond (T = Si or Al) of the zeolite Y. Figure 2 shows the calculated structure of the acidic zeolite Y at ONIOM (M062x/6-31G(d,p):PM6) level, with the T–O positions considered for insertion. Table 1 shows the energetic of methylene insertion in terms of enthalpy. All reactions are highly exothermic, indicating that insertion is favourable yielding a hybrid organic-zeolite structure. Triplet methylene is more stable than singlet methylene and this is reflected in the lower enthalpy difference for the insertion. All calculations intended to insert the carbene into the Al–O(2) bond (position B) afforded the methoxy group attached to the zeolite structure, indicating that insertion into the acidic O–H bond is preferred in this case. In fact, this was the most favourable pathway for the methylene insertion, presenting the highest enthalpy difference among all cases studied. However, when computing the insertion on the deprotonated zeolite Y this pathway was not observed, and the carbene was inserted into the Si(1)–O(1) bond. This result reflects the higher thermodynamic preference for insertion in the Si–O bond compared with the Al–O bond.

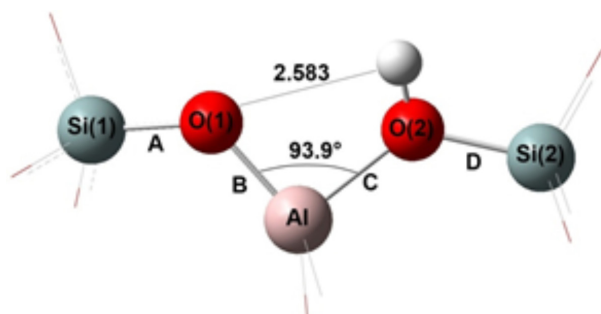


**Figure 2.** Calculated structure (H) of the acidic site of zeolite Y at ONIOM M062x/6-31G(d,p):PM6 (only the high layer shown) indicating the possible positions for carbene insertion into the zeolite Y framework.

The insertion of methylene leads to a local distortion of the structure to accommodate the carbenic moiety, with special modification in bond angles. Nevertheless,

**Table 1.** Calculated enthalpy difference of methylene ( $\text{CH}_2$ ) insertion into the framework T–O bond of zeolite Y at ONIOM (M062x/6-31G(d,p):PM6) level

T–O Bond	$\Delta H \text{ CH}_2$ (singlet) / (kcal mol <sup>-1</sup> )	$\Delta H \text{ CH}_2$ (triplet) / (kcal mol <sup>-1</sup> )
Si–O (A)	–64.0	–48.9
Al–O (B) <sup>a</sup>	–104.5	–89.3
Al–O (C)	–24.3	–9.2
Si–O (D)	–70.4	–55.2

<sup>a</sup>Calculations led to insertion into the acidic O–H bond, forming a methoxy group.

considering the limitations of the ONIOM method, one should see with care the flexibility in the zeolite framework. Table 2 shows some selected geometrical parameters for insertion in positions A, C and D in comparison with the geometry of the parent acidic zeolite Y (structure H). Figures 3-5 show the structures, highlighting the acid site neighbourhood, with some selected geometric data. Since insertion into Al–O(1) (structure B, not shown) led to a methoxy group, we did not include it in this comparison. As one can see, the parent acidic zeolite Y has the traditional geometry with Si–O bonds shorter than Al–O bonds. Insertion of methylene in the Si(1)–O(1) bond (structure A) did not significantly change the bond lengths. We observe a slight enlargement of the Al–O(1) bond and shrinkage of the Si(2)–O(2) bond to accommodate the  $\text{CH}_2$  moiety in the framework. The acidic O(2)–H bond is slightly longer than in the parent zeolite, but this is a result of the hydrogen bonding with the O(1) oxygen atom, which is not present in the parent zeolite (Figure 2). The greatest change in geometry was observed in the O(1)–Al–O(2) angle, which decreased from 93.9° in the parent acidic zeolite to 80.3° in structure A. The same behaviour was observed in structure D, computed for the insertion into the Si(2)–O(2) bond. The O(1)–Al–O(2) angle was 83.7° and there was a slight enlargement of the Al–O(1) bond and shrinkage of the Si(1)–O(1) bond in this structure. Finally, structure C, which represents the insertion in the Al–O(2) bond, shows minor modifications in the Si–O bond length compared with the acidic zeolite Y. The C–Al bond length is significantly longer than the computed Si–C bonds in structure A and D. The Al–C–O(2) angle of 125.4° is much larger than the tetrahedral angle observed for carbon atoms with  $\text{sp}^3$  hybridisation. These data suggest that the Al–C bond has some ionic character, with longer bond distance and larger bond angle than the Si–C bond.

After having observed that insertion of methylene into the framework Si–O bond is thermodynamically favoured, we studied the insertion of formylcarbene ( $\text{CHCHO}$ ) in the framework of zeolite Y. We considered

**Table 2.** Selected geometrical parameters of calculated structures of CH<sub>2</sub> insertion into zeolite Y framework at ONIOM (M062x/6-31G(d,p):PM6) level

Parameter/carbene insertion	H	A	C	D
Bond distances / Å				
Si(1)–O(1)	1.634	–	1.607	1.624
Al–O(1)	1.709	1.732	1.712	1.725
Al–O(2)	1.911	1.906	–	1.954
Si(2)–O(2)	1.719	1.683	1.753	–
O(2)–H	0.967	0.982	0.971	0.971
Si(1)–C	–	1.852	–	–
Si(2)–C	–	–	–	1.873
C–O(1)	–	1.416	–	–
C–O(2)	–	–	1.476	1.455
C–Al	–	–	1.973	–
Bond angles / degree				
Si(1)–O(1)–Al	125.1	–	127.0	123.4
O(1)–Al–O(2)	93.9	80.3	–	83.7
Al–O(2)–Si(2)	129.5	132.9	–	–
Si(1)–C–O(1)	–	109.7	–	–
C–O(1)–Al	–	111.2	–	–
O(1)–Al–C	–	–	84.7	–
Al–C–O(2)	–	–	125.4	–
C–O(2)–Si(2)	–	–	125.0	–
Al–O(2)–C	–	–	–	106.4
O(2)–C–Si(2)	–	–	–	110.5

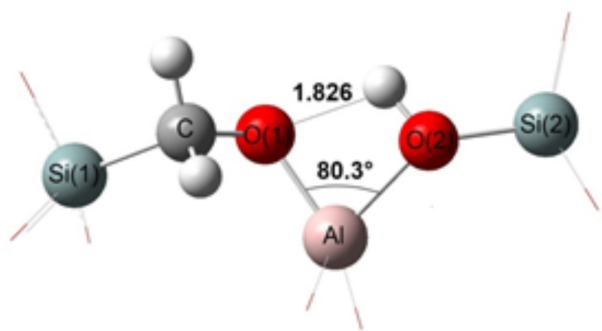


**Figure 3.** Calculated structure (A) of methylene insertion into the Si(1)–O(1) bond of zeolite Y at ONIOM (M062x/6-31G(d,p):PM6) (only the high layer shown).

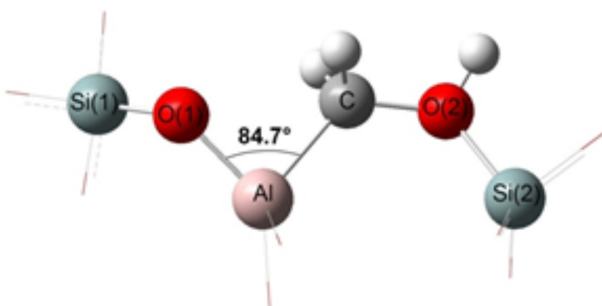


**Figure 4.** Calculated structure (C) of methylene insertion into the Al–O(2) bond of zeolite Y at ONIOM (M062x/6-31G(d,p):PM6) (only the high layer shown).

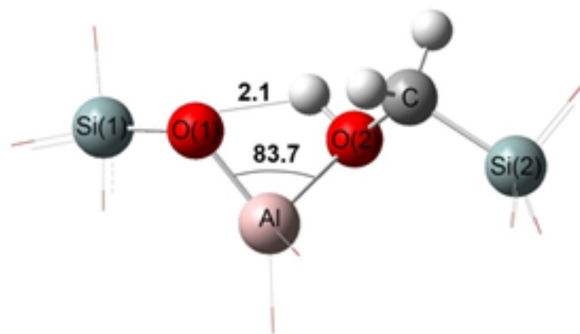


**Figure 5.** Calculated structure (D) of methylene insertion into the Si(2)–O(2) bond of zeolite Y at ONIOM (M062x/6-31G(d,p):PM6) (only the high layer shown).

only insertion in the Si–O bonds, as we have shown that it is thermodynamically more favourable than insertion into the Al–O bond. Because of the presence of two different substituents in the formylcarbene structure, the insertion may lead to the formation of two enantiomers, creating a chiral center (*R* or *S*) in the framework. We were able to calculate the thermodynamics only for the insertion of triplet formylcarbene, because the singlet species undergoes a rapid spin inversion to the most stable triplet state. The results are shown in Table 3. As in the case of methylene, insertion of formylcarbene in the zeolite framework is highly exothermic and thermodynamically favoured. The insertion into the Si(1)–O(1) bond is preferred, lying up to 14.3 kcal mol<sup>-1</sup> below in energy than insertion in the Si(2)–O(2) bond, depending on the enantiomer formed. The *E(R)* enantiomer is 1.4 kcal mol<sup>-1</sup> more stable than the *E(S)* isomer, whereas the *F(R)* enantiomer is 6.3 kcal mol<sup>-1</sup> lower in energy than the *F(S)* isomer. Table 4 and Figures 6 and 7 show some selected geometrical data of the *E* and *F* structures. The structure of enantiomers *E(R)* and *E(S)* are similar, and the main difference lies in the strength of the hydrogen bond between the proton and the carbonyl oxygen atom O(3). The shorter distance in *E(R)* may explain its lower energy. For the *F* enantiomers, the greatest geometric difference is in the O(1)–Al–O(2)–C(1) dihedral angle, which causes a significant local distortion in *F(R)*. For this enantiomer, the dihedral angle is 125.9°, whereas for the *F(S)* isomer the dihedral angle is 92.6°. The distortion may be related with the hydrogen bond in structure *F(R)*, where both O(1) and O(3) oxygen atoms interact with the acidic proton, stabilizing this enantiomer.

#### Acidity calculations

The acidity of the structures was calculated by means of the deprotonation energy and the results are shown in Table 5. We decided to consider only the structures with carbene insertion into the Si–O bond, because they

**Table 3.** Calculated enthalpy difference of formylcarbene (CHCHO) insertion into the framework Si–O bond of zeolite Y at ONIOM (M062x/6-31G(d,p):PM6) level

Structure/T–O bond	$\Delta H / (\text{kcal mol}^{-1})$
E( <i>R</i> )/Si(1)–O(1)	–54.0
E( <i>S</i> )/Si(1)–O(1)	–52.6
F( <i>R</i> )/Si(2)–O(2)	–46.0
F( <i>S</i> )/Si(2)–O(2)	–39.7

<sup>a</sup>(*R*) stands for the enantiomer with *R* configuration; <sup>b</sup>(*S*) stands for the enantiomer with *S* configuration.

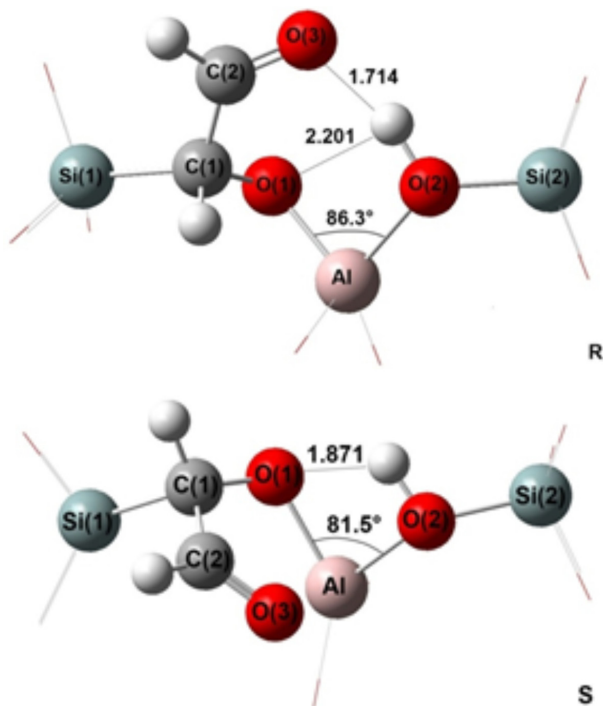


**Figure 6.** Calculated structure (E) of formyl carbene insertion into the Si(1)–O(1) bond of zeolite Y at ONIOM (M062x/6-31G(d,p):PM6) (only the high layer shown). *R* and *S* stand for the different enantiomers.

are significantly more favoured than the correspondent structures with insertion into the Al–O bond. In general, the structures formed upon the carbene insertion into the Si–O framework bonds are less acidic than the parent zeolite Y. Structures A and D, formed upon methylene insertion, have practically the same acidity, with an energy difference of 1.8 kcal mol<sup>–1</sup> favouring structure D. On the other hand, structures E and F, formed upon insertion of formylcarbene, have significantly different acidity, which also depends on the enantiomer configuration. Structure F is more acidic than structure E, with up to 17.2 kcal mol<sup>–1</sup> enthalpy difference, at ONIOM (M062x/6-31G(d,p):PM6) level, depending on the enantiomer considered. Indeed, the acidity of F(*S*) was slightly higher than the acidity of the parent protonic zeolite Y, inferring that carbene insertion may lead to stronger acid sites on the zeolite surface.

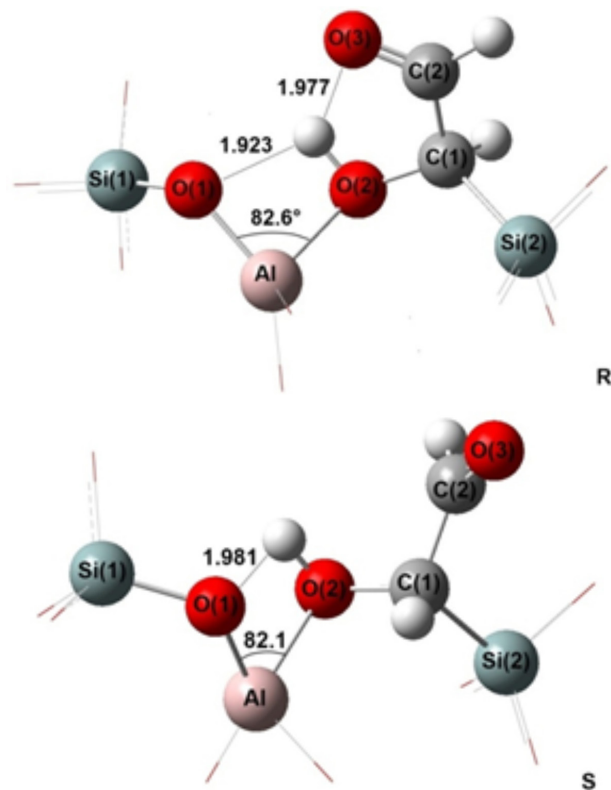


**Figure 7.** Calculated structure (F) of formyl carbene insertion into the Si(2)–O(2) bond of zeolite Y at ONIOM (M062x/6-31G(d,p):PM6) (only the high layer shown). *R* and *S* stand for the different enantiomers.

**Table 4.** Selected geometrical parameters of calculated structures of CH<sub>2</sub> insertion into zeolite Y framework at ONIOM (M062x/6-31G(d,p):PM6) level

Parameter/carbene insertion	E( <i>R</i> )	E( <i>S</i> )	F( <i>R</i> )	F( <i>S</i> )
Bond distances / Å				
Si(2)–O(2)	1.681	1.691	–	–
Si(1)–O(1)	–	–	1.626	1.619
Al–O(2)	1.885	1.910	1.992	1.918
Al–O(1)	1.714	1.802	1.727	1.716
O(2)–H	1.055	0.980	0.975	0.990
Si(1)–C	1.853	1.912	–	–
Si(2)–C	–	–	1.894	1.880
C–O(1)	1.389	1.371	–	–
C–O(2)	–	–	1.457	1.417
Bond angles / degree				
Si(1)–O(1)–Al	–	–	123.7	125.0
Si(2)–O(2)–Al(2)	123.9	130.6	–	–
O(1)–Al–O(2)	86.3	81.5	82.1	82.6
C(1)–O(1)–Al–O(2)	91.5	113.5	92.6	129.4

From the calculations, it is not completely clear the role of the carbenic moiety in the acid strength of the zeolite. The acidity was slightly reduced in relation to the

**Table 5.** Calculated deprotonation enthalpy of the parent acidic zeolite and the structures formed upon carbene insertion into the Si–O bond at ONIOM (M062x/6-31G(d,p):PM6) level

Structure	$\Delta H / (\text{kcal mol}^{-1})$
H <sup>a</sup>	295.4
A	300.8
D	299.0
E(R) <sup>b</sup>	310.9
E(S) <sup>b</sup>	312.3
F(R) <sup>b</sup>	297.9
F(S) <sup>b</sup>	293.7

<sup>a</sup>Protonic parent zeolite Y; <sup>b</sup>R and S stand for the enantiomer configuration.

parent protonic zeolite Y, except for the structure F(S). The formyl group has electron withdrawing properties and this may stabilize the conjugated base (deprotonated zeolite), helping increasing the acidity. Nevertheless, this effect was counterbalanced in structure F(R) due to the hydrogen bonding stabilisation on the protonated zeolite, which reduces the energy of the initial state (acidic form). Calculations indicated a change in the C–O(2) bond length upon deprotonation. It goes from 1.457 to 1.395 Å in F(S) and from 1.417 to 1.358 Å in F(R). This shrinkage of the bond may suggest that upon deprotonation, the excess of electrons in the oxygen atom may be delocalized on the organic moiety, stabilizing the conjugated base. Therefore, the main effect seems to be local, affecting the geometry and electronic density.

#### Expectations and practical considerations

Theoretical calculations have brought enormous advances in the understanding of catalyst structure and activity. In the case of zeolites, calculations helped understand the role of local<sup>34–36</sup> and long-range effects.<sup>37,38</sup> Most of the studies were carried out to explain experimental results, helping to create a general theory of zeolite acidity. Nevertheless, the development of heterogeneous acidic catalysts prior to their synthesis is still poorly explored in computational catalysis. This approach is common in drug discovery,<sup>39</sup> where computation may predict the biological activity of potential molecules, directing the synthesis and the commercialisation of new medicines. Although theory predicted that carbene insertion into the zeolite framework is thermodynamically favoured, there are some drawbacks to overcome if one wants to synthesize these structures for practical applications. Firstly, protonic zeolite may not be directly employed, because calculations pointed out to the formation of alkoxy species, upon insertion in the acidic O–H bond, as the most favourable pathway. To

circumvent this problem, one may use metal-exchanged zeolites, because calculations showed that in this case the insertion preferentially occurs in the Si–O bonds. It would also be interesting to explore the carbene insertion into pure silica zeolites thus, creating some functionalisation in these materials.

A potential analytical tool to characterize the carbene insertion into the zeolite is infrared spectroscopy, through the identification of some characteristic vibrational frequencies. The calculated stretching vibration for the CH<sub>2</sub> was 2965 cm<sup>-1</sup> (symmetric) and 3028 cm<sup>-1</sup> (asymmetric), whereas after insertion in the zeolite framework to form structure D the frequencies shift to 3094 cm<sup>-1</sup> (symmetric) and 3165 cm<sup>-1</sup> (asymmetric). In the case of formyl carbene, the stretching carbonyl vibration was calculated to be 1645 cm<sup>-1</sup>, whereas after insertion it varies from 1743 to 1890 cm<sup>-1</sup> depending on the enantiomer. This large shift may be explained in terms of the resonance of the carbene electron pair with the carbonyl group, which is not present after insertion in the zeolite framework.

Perhaps, the most interesting feature of the simulations of carbene insertion in the zeolite framework is the creation of chiral sites in the structure. Although chiral zeolite structures are known,<sup>40</sup> they do not normally induce asymmetric synthesis to produce enantiomeric excess. Chirality induction is normally described<sup>41</sup> as a local molecular event, requiring a chiral molecule or inductor. Although there are examples of asymmetric synthesis with zeolites,<sup>42</sup> the inclusion of a chiral inductor inside the cavities is normally required. Thus, zeolites are used mostly as a support for the chiral inductor, which could also be leached out upon several utilisations. The development of local chirality inside the zeolite pores is new and of high potential in the synthesis of drugs and fine chemical products. It may also be useful in biomass transformation, mimicking enzymes, which are both, catalysts and chiral inductors.

We have shown that insertion of formylcarbene affords enantiomers of different stability. Although we may not anticipate with these calculations if they would be experimentally produced in different amounts, one may expect that controlling the experimental conditions, as well as choosing the correct carbene structure, may favour the formation of the preferred enantiomer. The possibility of creating chiral sites in the zeolite framework may open a new era in zeolite catalysis, with the possibility of mimicking enzymes to produce pure enantiomers, or mixtures with high enantiomeric excess. The great advantage would be the higher thermal stability of the zeolites compared with the enzymes, allowing to work at higher temperatures to improve the kinetics.

There are few reports of carbene formation inside the zeolite cavity. Moya-Barrios and Cozens have studied<sup>43,44</sup> the formation and reaction of substituted arylcarbenes on metal-exchanged zeolite Y. They could follow the kinetics of formation and decay of the carbenes inside the zeolite by fluorescence analysis. They also proposed that the more electrophilic carbenes, such as chloro-*p*-nitrophenyl carbene, could undergo interaction with the zeolite structure to form alkoxides. This point is in agreement with calculations and suggest that carbenes of higher electrophilicity, such as carboxymethylcarbene, could eventually yield the insertion into the zeolite structure. Thus, the calculation is still waiting to be experimentally proven.

## Conclusions

Calculations show that insertion of carbenes into the T–O bond of the zeolite Y framework is thermodynamically favoured. Insertion in the Si–O bond is preferred over insertion in the Al–O bond, but the most favourable process is the insertion in the acidic O–H bond to form an alkoxide. Thus, the reaction should be attempted on cationic zeolites to avoid this latter pathway.

The insertion of formylcarbene introduces a chiral site in the framework, which may be potentially useful in asymmetric catalysis. The acidity of the zeolites, measured in terms of the deprotonation enthalpy, was slightly reduced in most of the structures formed upon carbene insertion. However, a specific enantiomer of formylcarbene insertion in the zeolite Si–O bond presented higher acid strength than the parent protonic zeolite. It is not completely clear the effect of the carbene moiety on the acid strength, but the results suggest that local effects, such as hydrogen bonding and electron withdrawing, may be of major importance.

The study of carbene insertion in the zeolite framework may lead to the design of new zeolite materials, modifying the acidity and creating chiral sites. These two features could mimic the behaviour of enzymes with the benefits of the higher thermal stability of the material, which would be able to work at higher temperatures.

## Acknowledgements

The authors acknowledge financial support from CNPq (process number 303718/2013-7) and FAPERJ (process number E-26/102772/2012).

## References

1. Corma, A.; *Chem. Rev.* **1995**, *95*, 559.

2. Weisz, P. B.; Miale, J. N.; *J. Catal.* **1965**, *4*, 527.  
 3. Miale, J. N.; Chen, N. Y.; Weisz, P. B.; *J. Catal.* **1966**, *6*, 278.  
 4. Barthomeuf, D.; Beaumont, R.; *J. Catal.* **1973**, *30*, 288.  
 5. Sohn, J. R.; DeCanio, S. J.; Fritz, P. O.; Lunsford, H. H.; *J. Phys. Chem.* **1986**, *90*, 4847.  
 6. Wang, Q. L.; Giannetto, G.; Guisnet, G.; *J. Catal.* **1991**, *130*, 471.  
 7. Keir, D.; Lee, E. F. T.; Rees, L. V. C.; *Zeolites* **1988**, *8*, 228.  
 8. Agudo, A. L.; Asensio, A.; Corma, A.; *J. Catal.* **1981**, *69*, 274.  
 9. Langenaeker, W.; Coussement, N.; De Profit, F.; Geerlings, P.; *J. Phys. Chem.* **1994**, *98*, 3010.  
 10. Parrillo, D. J.; Gorte, R. J.; *J. Phys. Chem.* **1993**, *97*, 8786.  
 11. Bahn, A.; Iglesia, E.; *Acc. Chem. Res.* **2008**, *41*, 559.  
 12. Umansky, B.; Engelhardt, J.; Hall, W. K.; *J. Catal.* **1991**, *177*, 128.  
 13. Xu, T. E.; Munson, J.; Haw, J. F.; *J. Am. Chem. Soc.* **1994**, *116*, 1962.  
 14. Gonçalves, V. L. C.; Rodrigues, R. C.; Lorençato, R.; Mota, C. J. A.; *J. Catal.* **2007**, *248*, 158.  
 15. Taarning, E.; Osmundsen, C. M.; Yang, X.; Voss, B.; Andersen, S. I.; Christensen, C. H.; *Energy Environ. Sci.* **2011**, *4*, 793.  
 16. van Santen, R. A.; Kramer, G. J.; *Chem. Rev.* **1995**, *95*, 637.  
 17. Asthagiri, A.; Janik, M.; *Computational Catalysis*; RSC: Cambridge, 2012.  
 18. Bhering, D. L.; Ramirez-Solis, A.; Mota, C. J. A.; *J. Phys. Chem. B* **2003**, *107*, 4342.  
 19. Suzuki, K.; Noda, T.; Sastre, G.; Katada, N.; Niwa, M.; *J. Phys. Chem. C* **2009**, *113*, 5672.  
 20. De Moor, B. A.; Reyniers, M. F.; Sierka, M.; Sauer, J.; Marin, G. B.; *J. Phys. Chem. C* **2008**, *112*, 11796.  
 21. Rigby, A. M.; Kramer, G. J.; van Santen, R. A.; *J. Catal.* **1997**, *170*, 1.  
 22. Boronat, M.; Viruela, P. M.; Corma, A.; *J. Am. Chem. Soc.* **2004**, *126*, 3300.  
 23. Fang, H.; Zheng, A.; Xu, J.; Li, S.; Chu, Y.; Chen, L.; Deng, F.; *J. Phys. Chem. C* **2011**, *115*, 7429.  
 24. Kazansky, V. B.; *Acc. Chem. Res.* **1991**, *24*, 379.  
 25. Tuma, C.; Kerber, T.; Sauer, J.; *Angew. Chem. Int. Ed.* **2010**, *49*, 1.  
 26. Bertrand, G.; *Carbene Chemistry: From Fleeting Intermediates to Powerful Reagents*; Marcel Dekker: New York, 2002.  
 27. Dapprich, S.; Komaromi, I.; Byun, K. S.; Morokuma, K.; Frisch, M. J.; *J. Mol. Struct.: THEOCHEM* **1999**, *462*, 1.  
 28. Sillar, K.; Burk, P.; *J. Phys. Chem. B* **2004**, *108*, 9893.  
 29. Rosenbach Jr., N.; dos Santos, A. P. A.; Franco, M.; Mota, C. J. A.; *Chem. Phys. Lett.* **2010**, *485*, 124.  
 30. Baerlocher, C. H.; Meier, W. M.; Olson, D. H.; *Atlas of Zeolite Framework Types*; Elsevier: Amsterdam, 2001.  
 31. Jirak, Z.; Vratilav, S.; Bosacek, V.; *J. Phys. Chem. Solids* **1980**, *41*, 1089.

32. Hill, J. R.; Freeman, C. R.; Delley, B.; *J. Phys. Chem. A* **1999**, *103*, 3772.
33. Frisch, M. J.; Trucks, G. W.; Schlegel, H. B.; Scuseria, G. E.; Robb, M. A.; Cheeseman, J. R.; Scalmani, G.; Barone, V.; Mennucci, B.; Petersson, G. A.; Nakatsuji, H.; Caricato, C.; Li, X.; Hratchian, H. P.; Izmaylov, A. F.; Bloino, J.; Zheng, G.; Sonnenberg, J. L.; Hada, M.; Ehara, M.; Toyota, K.; Fukuda, R.; Hasegawa, J.; Ishida, M.; Nakajima, T.; Honda, Y.; Kitao, O.; Nakai, H.; Vreven, T.; Montgomery, J. A.; Peralta, J. E.; Ogliaro, F.; Bearpark, M.; Heyd, J. J.; Brothers, E.; Kudin, K. N.; Staroverov, V. N.; Kobayashi, R.; Normand, J.; Raghavachari, K.; Rendell, A.; Burant, J. C.; Iyengar, S. S.; Tomasi, J.; Cossi, M.; Rega, N.; Millam, J. M.; Klene, M.; Knox, J. E.; Cross, J. B.; Bakken, V.; Adamo, C.; Jaramillo, J.; Gomperts, R.; Stratmann, R. E.; Yazyev, O.; Austin, A. J.; Cammi, R.; Pomelli, C.; Ochterski, J. W.; Martin, R. L.; Morokuma, K.; Zakrzewski, V. G.; Voth, V. A.; Salvador, P.; Dannenberg, J. J.; Dapprich, S.; Daniels, A. D.; Farkas, O.; Foresman, J. B.; Ortiz, J. V.; *GAUSSIAN 09, Revision A.2*; Gaussian Inc.: Wallingford, CT, USA, 2009.
34. Gonzales, N. O.; Bell, A. T.; Chakraborty, A. K.; *J. Phys. Chem. B* **1997**, *101*, 10058.
35. Vayssilov, G. N.; Rosch, N.; *J. Phys. Chem. B* **2001**, *105*, 4277.
36. Xu, B.; Sievers, C.; Hong, S. B.; Prins, R.; van Bokhoven, J. A.; *J. Catal.* **2006**, *244*, 163.
37. Rozanska, X.; Barbosa, L. A. M. M.; van Santen, R. A.; *J. Phys. Chem. B* **2005**, *109*, 2203.
38. Tuma, C.; Sauer, J.; *Phys. Chem. Chem. Phys.* **2006**, *8*, 3955.
39. Bultinck, P.; De Winter, H.; Langenaeker, W.; Tollenare, J. P.; *Computational Medicinal Chemistry for Drug Discovery*; Marcel Dekker: New York, 2003.
40. Sun, J.; Bonneau, C.; Cantín, A.; Corma, A.; Díaz-Cabañas, M. J.; Moliner, M.; Zhang, D.; Li, M.; Zou, X.; *Nature* **2009**, *458*, 1154.
41. Saigo, K.; Hashimoto, Y.; Kinbara, K.; Sudo, A.; *J. Chem. Sci.* **1996**, *108*, 555.
42. Willock, D. J.; Bethell, D.; Feast, S.; Hutchings, G. J.; King, F.; *Top. Catal.* **1996**, *3*, 77.
43. Moya-Barrios, R.; Cozens, F. L.; *Org. Lett.* **2004**, *6*, 881.
44. Moya-Barrios, R.; Cozens, F. L.; *J. Am. Chem. Soc.* **2006**, *128*, 14836.

Submitted: December 19, 2013  
Published online: April 11, 2014